Icarus 206 (2010) 189–198

Contents lists available at ScienceDirect

Icarus

journal homepage: www.elsevier.com/locate/icarus

Search for Phobos and Deimos gas/dust tori using in situ observations from Mars Global Surveyor MAG/ER

Marit Øieroset [a,*], David A. Brain [a], Erin Simpson [a], David L. Mitchell [a], Tai D. Phan [a], Jasper S. Halekas [a], Robert P. Lin [a], Mario H. Acuña [b,1]

[a] Space Sciences Laboratory, University of California, Berkeley, CA 94720, USA
[b] Goddard Space Flight Center, Greenbelt, Maryland

ARTICLE INFO

Article history:
Received 21 November 2008
Revised 4 June 2009
Accepted 16 July 2009
Available online 25 July 2009

Keywords:
Mars, Satellites
Planetary rings
Solar wind

ABSTRACT

More than 490 elliptical aerobraking and science phasing orbits made by Mars Global Surveyor (MGS) in 1997 and 1998 provide unprecedented coverage of the solar wind in the vicinity of the orbits of the martian moons Phobos and Deimos. We have performed a comprehensive survey of magnetic field perturbations in the solar wind to search for possible signatures of solar wind interaction with dust or gas escaping from the moons. A total of 1246 solar wind disturbance events were identified and their distribution was examined relative to Phobos, the Phobos orbit, and the Deimos orbit. We find that the spatial distribution of solar wind perturbations does not increase near or downstream of Phobos, Phobos' orbit, or Deimos' orbit, which would have been expected if there is significant outgassing or dust escape from the martian moons. Of the 1246 magnetic field perturbation events found in the MGS data set, 11 events were found within 2000 km of the Phobos orbit, while three events were found within 2000 km of the Deimos orbit. These events were analyzed in detail and found to likely have other causes than outgassing/dust escape from the martian moons. Thus we conclude that the amount of gas/dust escaping the martian moons is not significant enough to induce detectable magnetic field perturbations in the solar wind. In essence we have not found any clear evidence in the MGS magnetic field data for outgassing or dust escape from the martian moons.

1. Introduction

It has long been suspected that Mars is encircled by two faint gas/dust rings, one originating from each of its moons Phobos and Deimos (Soter, 1971). Phobos and Deimos have mean radii of 6.2 km and 11.1 km, respectively. Gas/dust belts along the orbits of the martian satellites can be maintained by meteorite impacts on the satellite surfaces, by outgassing, or by interaction with the hot oxygen corona of Mars (Soter, 1971; Ip and Banaszkiewicz, 1990). Early in situ observations from Mars-5 downstream of Deimos suggested that Deimos was outgassing and hence interacting with the solar wind (Bogdanov, 1981).

Furthermore, the Phobos-2 mission reported the possible in situ detection of magnetic field and plasma signatures caused by the presence of gas and dust forming a ring or torus along the orbit of the martian moon Phobos (Riedler et al., 1989; Dubinin et al., 1990). These Phobos events were characterized by magnetic field magnitude fluctuations up to 4 nT accompanied by electron density increases. Phobos-2 came within 700 km of the Phobos orbit during each of its first three elliptical orbits and recorded a magnetic field fluctuation each time. The Phobos-2 observations of possible outgassing/dust escape from Phobos and associated models have been discussed in detail by Mazelle et al. (2004).

However, despite the coincidence with Phobos orbit crossings of three discrete plasma disturbances detected by the Phobos-2 spacecraft, Russell et al. (1990) pointed out that foreshock turbulence could also be responsible for the Phobos events. This latter hypothesis was supported by the magnetic field geometry showing magnetic connection to the bow shock during the events in question. Russell et al. (1990), and later Dubinin et al. (1995), also noted the similarity between one of the Phobos events and so-called hot diamagnetic cavities (later termed hot flow anomalies (HFAs)) which had been observed upstream of the Earth's bow shock (Schwartz et al., 1985; Thomsen et al., 1986). Attempts to trace the Phobos and Deimos rings by optical means have so far been unsuccessful (Duxbury and Ocampo, 1988; Showalter et al., 2006).

Thus the source of the Phobos events remains a controversial topic which could not easily be resolved with the limited data set from the Phobos-2 spacecraft. In this paper we present a comprehensive search for Phobos and Deimos gas/dust torus events using the MGS magnetometer (MAG) data from 493 MGS elliptical aerobraking and science phasing orbits.

* Corresponding author. Fax: +1 510 643 8302.
E-mail address: oieroset@ssl.berkeley.edu (M. Øieroset).
[1] Deceased.

0019-1035/$ - see front matter © 2009 Elsevier Inc. All rights reserved.
doi:10.1016/j.icarus.2009.07.017

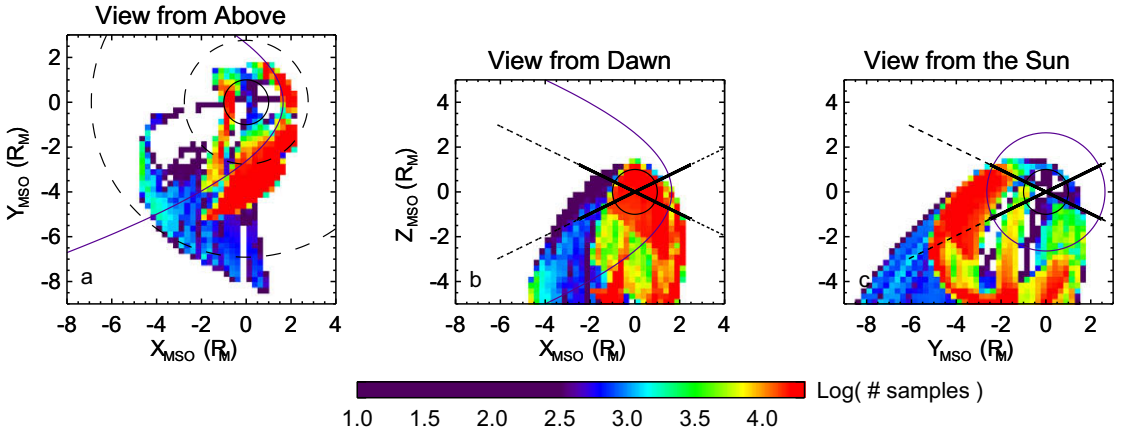

Fig. 1. MGS SPO and AB orbit coverage in the Mars-centered Solar Orbital (MSO) coordinate system. In the MSO coordinate system +*X* is sunward from the center of the planet, the +*Y* direction is duskward, and the +*Z* direction toward the north ecliptic pole. The color bar denotes the total number of magnetic field vectors recorded by MGS. (a) MGS orbit coverage projected onto the *X*–*Y* plane; (b) MGS orbit coverage projected onto the *X*–*Z* plane; (c) MGS orbit coverage projected onto the *Y*–*Z* plane. The bow shock as well as the northward and southward extremes of the Phobos (solid line) and Deimos (dashed line) orbit projections in each plane are marked. (For interpretation of the references to color in this figure legend, the reader is referred to the web version of this article.)

2. Instrumentation and data coverage

We use magnetic field data from the magnetometer/electron reflectometer (MAG/ER) experiment (Acuña et al., 1998) onboard the MGS spacecraft. The magnetic field vector sample rate used in this study varies between 0.75 s, 1.5 s, and 3 s.

The data were collected during 493 aerobraking (AB) and science phasing orbits (SPO) between September 14, 1997 and September 17, 1998 when MGS sampled the solar wind upstream of the martian bow shock in the vicinity of Phobos, Deimos, and their orbits repeatedly. Fig. 1 shows the MGS AB and SPO orbit coverage. MGS spent more than 20 h within 2000 km of both Phobos' and Deimos' orbit. The majority of samples were obtained in the pre-noon local time sector, while the coverage is sparse north of the ecliptic plane and in the dusk sector.

In this study we use the Mars-centered Solar Orbital (MSO) coordinate system. In the MSO coordinate system +*X* is sunward from the center of the planet, the +*Y* direction is duskward, and the +*Z* direction toward the north ecliptic pole.

3. Observations

Although there are presently no commonly accepted theoretical predictions of the magnitude of magnetic perturbation expected from the Phobos and Deimos gas/dust torus, at least two candidate generation mechanisms have been suggested.

First, Krymskii et al. (1992) postulated that if gas/dust is present along the Phobos and Deimos orbits it would be positively charged by photo-ionization and electrons would be attracted to balance the charge density. The resulting motion of electrons with respect to protons would lead to low frequency MHD fluctuations in the vicinity of the moons' orbits.

Ip and Banaszkiewicz (1990) proposed an alternative generation mechanism in which pickup-ions from the putative Phobos gas torus and oppositely moving photoelectrons would constitute a so-called pickup current in the mass loading region. Baumgärtel et al. (1998) proposed that the newly formed heavy ions could form a ring-beam like pitch angle distribution in the solar wind frame, giving rise to a variety of low frequency electromagnetic instabilities with large amplitudes, and therefore possibly explain the Phobos-2 Phobos events. Waves induced by pickup-ions have been observed near Io (Russell and Kivelson, 2000; Blanco-Cano et al., 2001; Cowee et al., 2007) and in the region of the E ring at Saturn (Russell and Blanco-Cano, 2007). Water-group pickup-ions have been detected in the Enceladus torus (Tokar et al., 2006).

In addition to the events reported near the Phobos orbit (Riedler et al., 1989; Dubinin et al., 1990) it has been suggested that outgassing from the martian moons could give rise to Mach cones downstream of the moons (Sauer et al. (1995)). Thus if outgassing from Phobos and Deimos were indeed giving rise to detectable magnetic field signatures in the solar wind one would expect to find these events in the vicinity of the moons' orbits (either due to the Krymskii et al. (1992) or the Baumgärtel et al. (1998) mechanisms outlined above) or downstream of the moons and their orbits (due to the Mach cones induced from the gas/dust).

Without making any assumption about which mechanism could be responsible for the Phobos-2 Phobos events we have searched the MGS AB and SPO data set for magnetic field fluctuation events similar to those reported by Phobos-2 (Riedler et al., 1989; Dubinin et al., 1990). We limited the search to times when MGS was upstream of the martian bow shock, i.e. in the solar wind.

3.1. Statistical study of solar wind disturbance events

We selected events characterized by strong fluctuations in the magnetic field. This was accomplished by calculating a running "rms ratio", the ratio of the local rms to its mean value, and then selecting events where the rms ratio exceeded a minimum value of 3.0. The local rms is the root mean square deviation of the magnetic field magnitude from its running average value calculated within a 30 s interval. The mean of the local rms is a running average of the local rms calculated within a 1200 s interval. The 3.0 rms ratio value was chosen because with this rms ratio most of the selected events resembled the Phobos-2 Phobos events. Smaller rms ratios of 2.0 and 2.5 were also tried and yielded similar results. The times and durations of the events, as well as the MSO coordinates of all data points within each event were recorded. A total of 1246 events were identified by the algorithm.

Examples of the types of events identified by this algorithm are shown in Fig. 2. Fig. 2a shows a ~3 min magnetic field fluctuation with an amplitude of 2–3 nT recorded on October 19, 1997, while Fig. 2b shows two events with brief depressions of 2–3 nT in magnetic field magnitude observed on November 19, 1997. The event in Fig. 2a was recorded 29,600 km and 32,400 km from the Phobos and Deimos orbits, respectively. The second event shown in Fig. 2b was observed 31,200 km and 31,400 km from the Phobos and

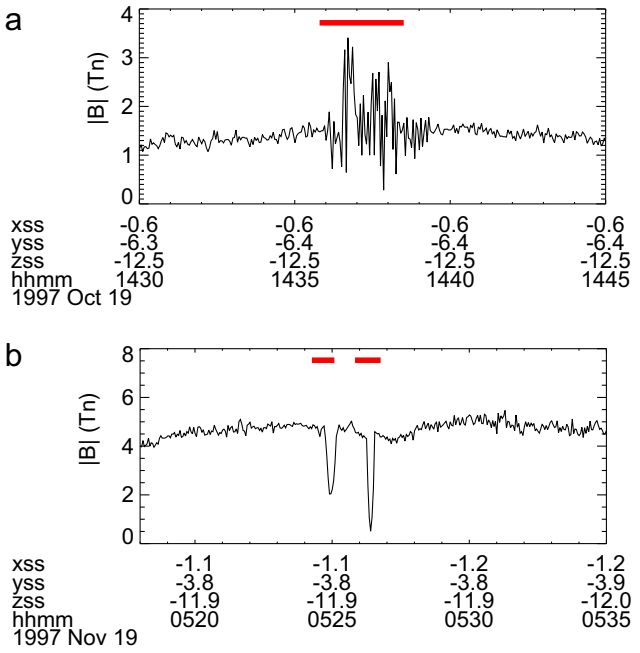

Fig. 2. Example of solar wind disturbance events identified by the automated algorithm described in Section 3.1. The events are marked with the red bars. (a) MGS magnetic field observations from October 19, 1997. (b) MGS magnetic field observations from November 19, 1997. These two events were recorded far (>29,000 km) from the Phobos and Deimos orbits. (For interpretation of the references to color in this figure legend, the reader is referred to the web version of this article.)

Deimos orbits, respectively. Hence the events displayed in Fig. 2 are observed far away from the Phobos and Deimos orbits, but still closely resemble the Phobos 2 Phobos events (Riedler et al., 1989; Dubinin et al., 1990).

The 1246 events were sorted into bins based on their directional (*dx*, *dy*, *dz* – see below for definitions of the coordinate systems used) and total distance from Phobos and Deimos and their orbits. Each distance bin was 1000 km wide and the event probability was calculated for each bin. Showalter et al. (2006) estimated the thickness of the Deimos gas/dust ring to be as large as 6000 km for 40 mm particles. The Phobos ring was suggested to extend to several 1000 km (Baumgartel et al., 1998). Thus in our study we consider events detected within a distance of 10,000 km from Phobos, Phobos orbit, and Deimos orbit (Figs. 3–5). The event probability near Deimos is not considered in this study since the MGS coverage is too sparse near Deimos. The error bars in Figs. 3–5 reflect assumed Poisson error in the number of events in each bin.

If outgassing/dust escape from the martian moons were to provide measurable magnetic field signatures outside the bow shock we would expect to see a peak in event occurrence near or downstream of Phobos, Phobos' orbit, or Deimos' orbit. Magnetic signatures of the putative gas torus could be observable a few hundred km away from the moons' orbits, depending on the mass of the neutrals present in the torus. Assuming that the moon is emitting oxygen which is then ionized and picked up by the solar wind (e.g., Baumgärtel et al., 1998), the O^+ gyro radius of at least a few hundred km could lead to observable magnetic field signatures of the putative gas torus a few hundreds of km away from the moons' orbits. In addition to the magnetic signatures generated by the pickup-ions in the torus itself, the gas or dust around the moons and/or in their orbits could lead to Mach cones in the solar wind downstream of the moons and/or their orbits. However, no peaks in the event distribution are observed near or downstream of the martian moons or their orbits as we now describe.

Figs. 3–5 display the event occurrence frequency (a–d), the coverage (crosses in panels e–h), and the number of events (diamonds in panels e–h) as a function of *dx*, *dy*, *dz*, and total distance from the Phobos moon, the Phobos orbit, and the Deimos orbit, respectively. Only events within 10,000 km of Phobos, Phobos' orbit, and Deimos' orbit, respectively, are included. The coverage is given in number of magnetic field vectors measured (MGS MAG temporal resolution varies between 0.75, 1.5, and 3.0 s) in each 1000 km bin. The distances *dx*, *dy*, *dz*, and total distance are measured from the center of Phobos (Fig. 3), or from the point along the Phobos or Deimos orbit which was closest to MGS at the time when the event was observed (Figs. 4 and 5). In Fig. 3 positive *dx* points from Phobos toward the Sun, positive *dy* points duskward, and positive *dz* points toward the north ecliptic pole. In Figs. 4 and 5 positive *dx* points from the closest approach point in the Phobos/Deimos orbit toward the Sun, positive dy points duskward, and positive *dz* points toward the north ecliptic pole.

3.1.1. Event frequency as a function of distance from Phobos

The event probability is similar for negative and positive *dx* (Fig. 3a), thus there is no preference for events to be located behind the Phobos moon, which would be expected if there is significant outgassing or dust escape from Phobos. The vast majority of events are observed for negative *dy* (Fig. 3f) and negative *dz* (Fig. 3g), giving rise to higher event probabilities in these regions (Fig. 3b and c).

The event probability increases with increasing total distance from Phobos (Fig. 3d), which is opposite to what is expected if there is significant outgassing or dust escape from the moon. Fig. 3h shows that MGS did not spend any time in the 0–1000 km bin, but did spend ~1 h in the 1000–2000 km bin. However, no events were observed in the 1000–2000 km bin. Zero and one events were recorded in the 2000–3000 km bin and the 3000–4000 km bin, respectively. Two events were recorded in the 4000–5000 km bin. The occurrence frequency stayed below 0.0002 for all distances (0–10,000 km).

Table 1 shows the probability values derived from χ^2 analysis for each *dx*, *dy*, *dz*, and total distance data set. The values suggest that the events are not drawn randomly from the distribution in coverage. Thus despite the low number of events in some bins the probabilities are statistically significant. The χ^2 analysis is described below in Section 3.1.4.

3.1.2. Event frequency as a function of distance from the Phobos orbit

There appears to be an increase in event probability behind the Phobos orbit centered at $dx = -5000$ km (Fig. 4a). However, in Fig. 4e it can be seen that in fact only three events were observed in each of these bins. In fact, the event probability is higher in the $dx = (0, 2000$ km) bins (i.e., sunward of the Phobos orbit) than in the $dx = (-2000, 0)$ bins (anti-sunward of the Phobos orbit), based on tens of events observed in these bins (Fig. 4a and e). Thus we conclude that there is no preference for events to occur anti-sunward or sunward of the Phobos orbit.

Table 1
Probability that events are random for the event distribution relative to the Phobos moon.

Distribution	Probability
dx	23.95
dy	58.10
dz	8.15
Total distance	0.04

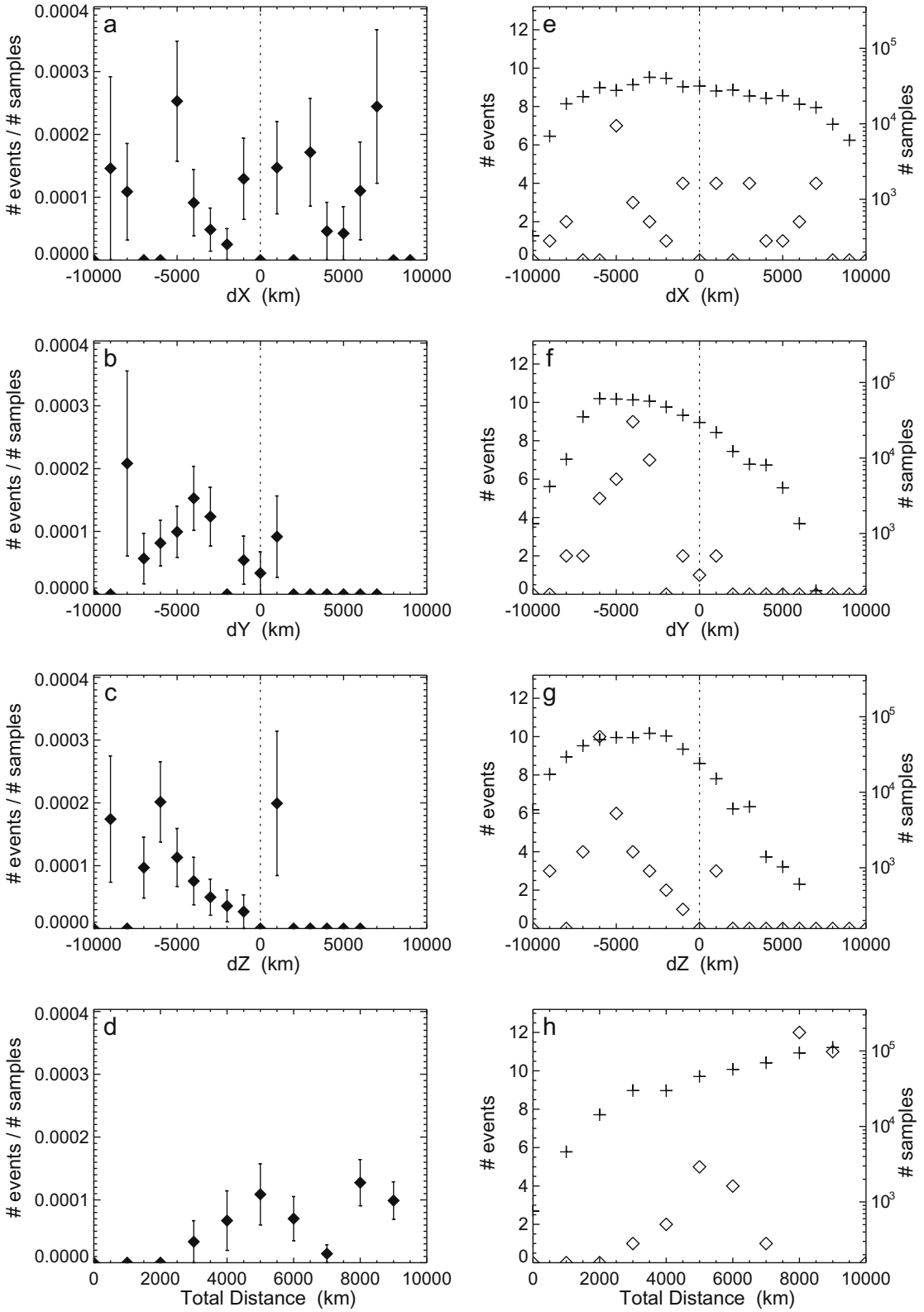

Fig. 3. Results from the search for solar wind disturbance events relative to Phobos: (a) event probability (number of events divided by number of samples) as a function of *dx*; (b) event probability as a function of *dy*; (c) event probability as a function of *dz*; (d) event probability as a function of total distance; (e) number of events (diamonds) and number of samples (crosses) as a function of *dx*; (f) number of events (diamonds) and number of samples (crosses) as a function of *dy*; (g) number of events (diamonds) and number of samples (crosses) as a function of *dz*; (h) number of events (diamonds) and number of samples (crosses) as a function of total distance. The (*dx*, *dy*, *dz*) is the Phobos-centered coordinate system where *dx* points toward the Sun, *dy* toward dusk, and *dz* toward the north ecliptic pole. The number of samples are given as number of magnetic field vectors measured (MGS MAG temporal resolution varies between 1.5 and 3 s). See text for an explanation of the error bars.

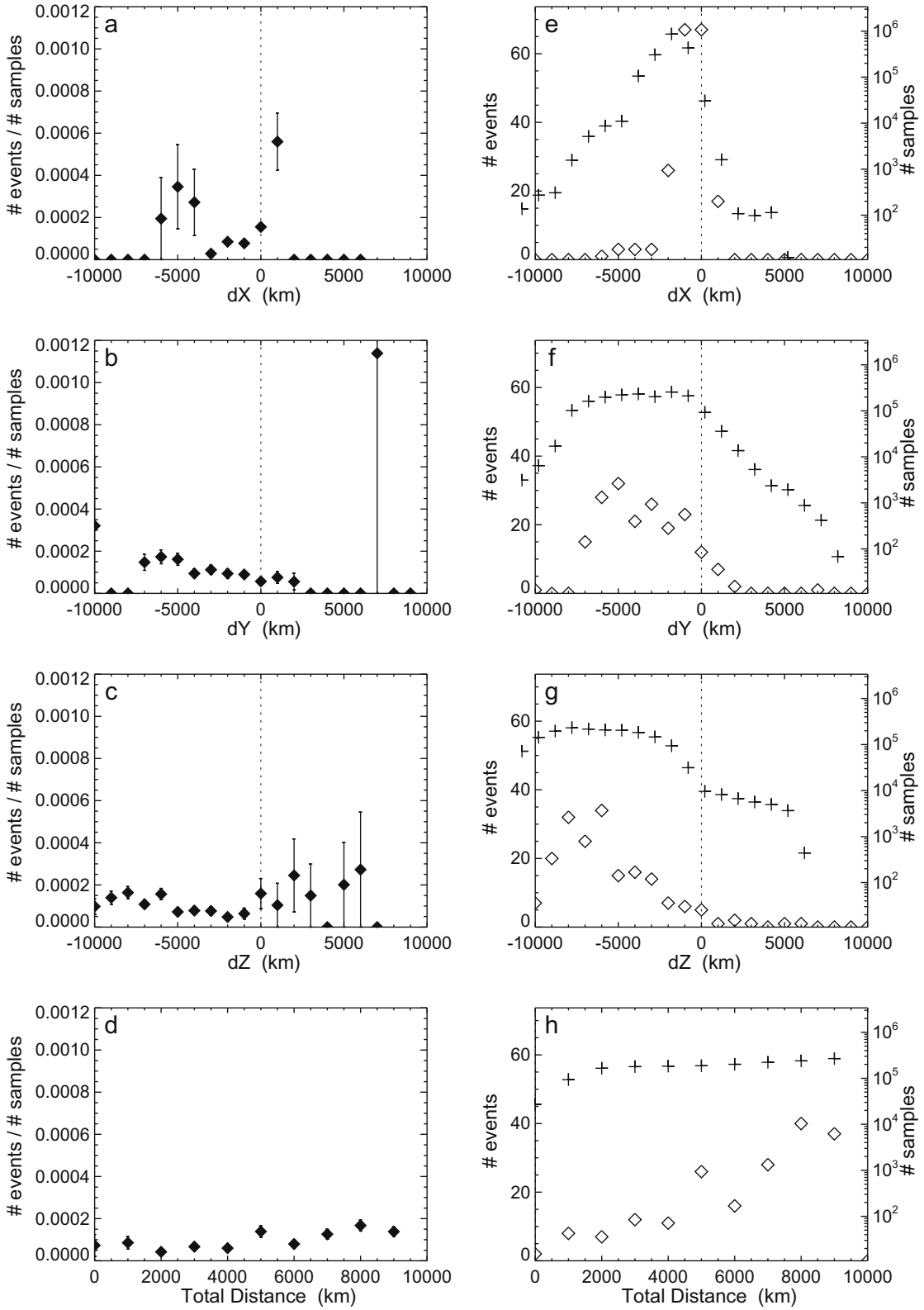

Fig. 4. Results from the search for solar wind disturbance events relative to the Phobos orbit: (a) event probability (number of events divided by number of samples) as a function of *dx*; (b) event probability as a function of *dy*; (c) event probability as a function of *dz*; (d) event probability as a function of total distance; (e) number of events (diamonds) and number of samples (crosses) as a function of *dx*; (f) number of events (diamonds) and number of samples (crosses) as a function of *dy*; (g) number of events (diamonds) and number of samples (crosses) as a function of *dz*; (h) number of events (diamonds) and number of samples (crosses) as a function of total distance. The (*dx*, *dy*, *dz*) coordinate system is centered in the point along the Phobos orbit which is closest to MGS at the time of the measurement. The *dx* points toward the Sun, *dy* toward dusk, and *dz* toward the north ecliptic pole. The number of samples are given as number of magnetic field vectors measured (MGS MAG temporal resolution varies between 1.5 and 3 s). See text for an explanation of the error bars.

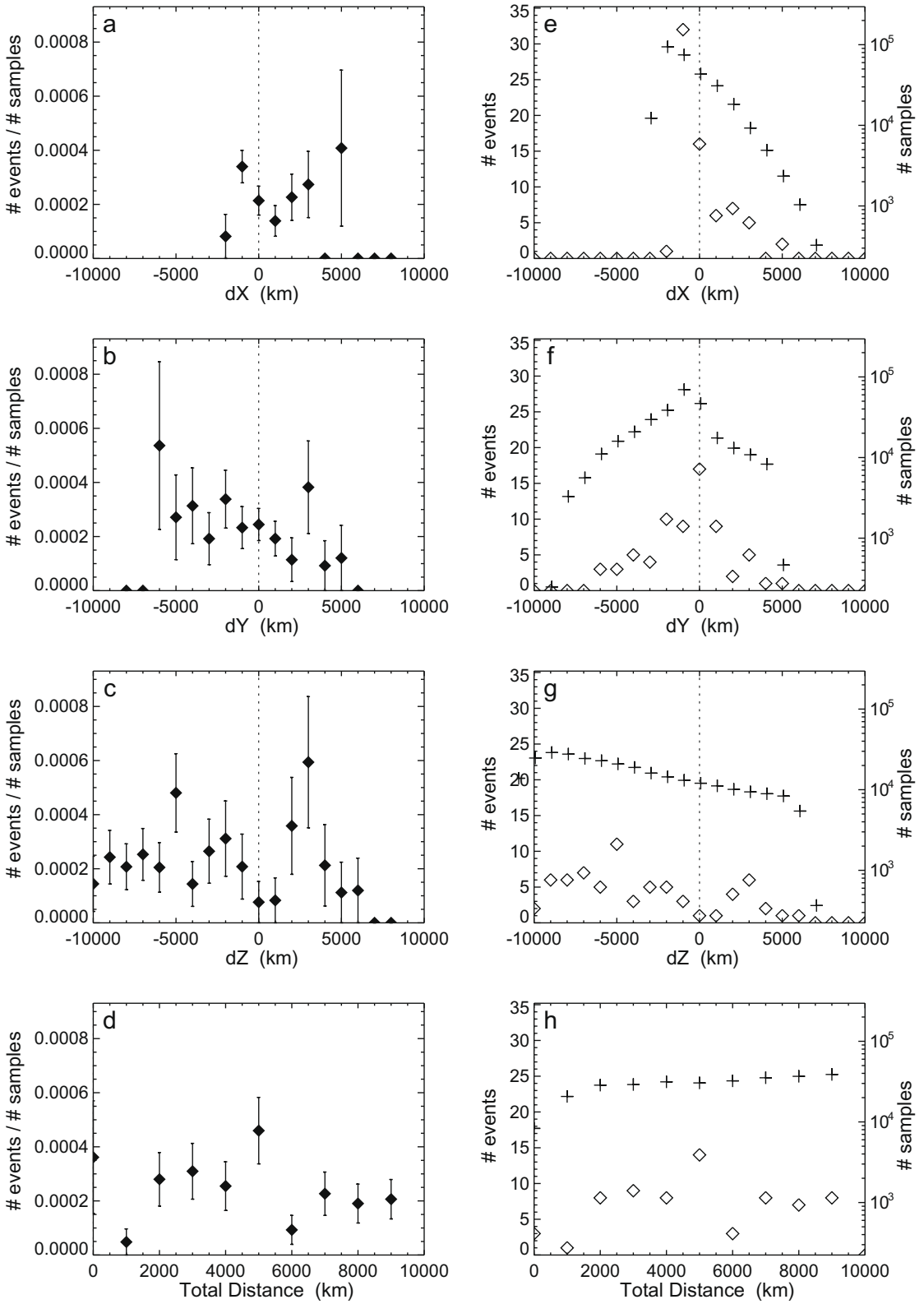

Fig. 5. Results from the search for solar wind disturbance events relative to the Deimos orbit: (a) event probability (number of events divided by number of samples) as a function of *dx*; (b) event probability as a function of *dy*; (c) event probability as a function of *dz*; (d) event probability as a function of total distance; (e) number of events (diamonds) and number of samples (crosses) as a function of *dx*; (f) number of events (diamonds) and number of samples (crosses) as a function of *dy*; (g) number of events (diamonds) and number of samples (crosses) as a function of *dz*; (h) number of events (diamonds) and number of samples (crosses) as a function of total distance. The (*dx*, *dy*, *dz*) coordinate system is centered in the point along the Deimos orbit which is closest to MGS at the time of the measurement. The *dx* points toward the Sun, *dy* toward dusk, and *dz* toward the north ecliptic pole. The number of samples are given as number of magnetic field vectors measured (MGS MAG temporal resolution varies between 1.5 and 3 s). See text for an explanation of the error bars.

Table 2
Probability that events are random for the event distribution relative to the Phobos orbit.

Distribution	Probability
dx	0.00
dy	1.42
dz	0.90
Total distance	0.00

As was the case for the Phobos moon (Section 3.1.1) the event probability is higher for negative *dy* (Fig. 4b). The event probability is relatively similar for negative and positive *dz*, although the error bars are large for positive dz due to the small number of events observed there (Fig. 4g).

Fig. 4d and h show the event occurrence frequency, the total observation time, and the number of events as a function of total distance from the Phobos orbit. The coverage was good in all bins, including the bins closest to the Phobos orbit, with ~6 h of observation time in the 0–1000 km bin and 20 h of observation time in the 1000–2000 km bin. Eleven events were identified within 2000 km of the Phobos orbit (Fig. 4h). The occurrence frequency is rather constant with total distance (Fig. 4d) and no increase in event frequency was seen in the bins closest to the Phobos orbit. The event frequency remained below 0.0002 in all bins. The eleven events observed within 2000 km of the Phobos orbit are examined in Section 3.2 below.

Table 2 shows the probability values derived from χ^2 analysis for each *dx*, *dy*, *dz*, and total distance data set. The values suggest that the events are not drawn randomly from the distribution in coverage. Thus despite the low number of events in some bins the probabilities are statistically significant. The χ^2 analysis is described below in Section 3.1.4.

3.1.3. Event frequency as a function of distance from the Deimos orbit

Fig. 5a shows that the event probabilities are similar sunward and anti-sunward of the Deimos orbit. Also, the event probabilities are similar for positive and negative *dy* and *dz*. Thus there appear to be no directional dependence.

Fig. 5d and h show the event occurrence frequency, the total observation time, and the number of events as a function of total distance from the Deimos orbit. The coverage was good in all bins, including the bins closest to the Deimos orbit, with ~7 h of observation time in the 0–1000 km bin and nearly 20 h of observation time in the 1000–2000 km bin. Three events were observed within 2000 km from the Deimos orbit, with two events in the 0–1000 km bin and one event in the 1000–2000 km bin (Fig. 3h). These three events are examined below (Section 3.2). No particular trend is seen in the event probability as a function of total distance (Fig. 5d).

Table 3 shows the probability values derived from χ^2 analysis for each *dx*, *dy*, *dz*, and total distance data set. The values suggest that the events are not drawn randomly from the distribution in coverage. Thus despite the low number of events in some bins the probabilities are statistically significant. The χ^2 analysis is described below in Section 3.1.4.

Table 3
Probability that events are random for the event distribution relative to the Deimos orbit.

Distribution	Probability
dx	11.78
dy	59.61
dz	31.00
Total distance	0.12

3.1.4. χ^2 analysis

To investigate whether the results displayed in Figs. 3–5 are statistically significant we have performed a χ^2 analysis. χ^2 is defined as

$$\chi^2 = \frac{1}{(N-1)} \sum_{i=1}^{n} \frac{(N_1 - N_2)^2}{\sigma^2} \quad (1)$$

where N is the number of bins, N_1 is the normalized coverage (total number of magnetic field vectors), N_2 is the normalized number of events, and σ is the standard deviation. The degrees of freedom is $(N-1)$ since N_1 and N_2 are normalized. We have excluded the bins where zero events were observed. The χ^2 values were then converted into significance levels, indicating the probability that the distribution of high RMS events was drawn randomly from the MGS measurements.

Tables 1–3 show these probabilities for the Phobos, Phobos' orbit, and Deimos' orbit event probability distributions in *dx*, *dy*, *dz*, and total distance. The smaller the probability is the more likely it is that the distribution of high RMS events was not drawn randomly from the distribution. The probabilities are relatively small for all probability distributions. Thus the preference for events to occur for negative dy relative to Phobos (Fig. 3b) and Phobos' orbit (Fig. 4b) is likely a real effect. This behavior is likely not associated with Phobos itself, since if outgassing/dust escape from Phobos were to provide measurable magnetic field signatures we would expect to see a peak in event occurrence near or downstream of Phobos or Phobos' orbit (i.e., in *dx* and not in *dy*), and such peaks are not seen. The preference for events to occur for negative *dy* could be related to the foreshock being preferably located on the dawn side, giving rise to more events in this sector. As can be seen in Fig. 1 parts of the Phobos and Deimos orbits are located in the foreshock. We do indeed expect the event probability to peak in the martian foreshock, i.e., it is not surprising that the χ^2 test indicates that the events are not randomly distributed in space.

The preference for events to occur for negative *dz* relative to the Phobos moon (Fig. 3c) could be related to the MGS orbit. Whenever MGS is in the dawn sector (i.e., the foreshock) the MGS orbit is such that *dz* is mostly negative, giving rise to the higher event probabilities for negative *dz*.

In summary, the results displayed in Figs. 3–5 show that there is no preference for events to occur in the vicinity of Phobos, the Phobos orbit, or the Deimos orbit. Also, there is no clustering of events anti-sunward of Phobos, Phobos' orbit, or Deimos' orbit which would be expected if there is significant outgassing or dust escape from the martian moons. However, although the event probabilities stayed relatively constant with distance, a small number of events were indeed found in the vicinity of the moons' orbits and below we examine them in detail.

3.2. Events found in the vicinity of the moons' orbits

The Phobos-2 Phobos events were recorded within 700 km from the Phobos orbit (Riedler et al., 1989; Dubinin et al., 1990). In the statistical search for events described above we found eleven solar wind disturbance events within 2000 km of the Phobos orbit and three such events within 2000 km of the Deimos orbit. We now examine these events in detail.

3.2.1. Candidate "Phobos events"

Eleven events were identified within 2000 km of the Phobos orbit. Seven of the events exhibited large magnetic field magnitude increases at spacecraft locations consistent with a crossing of the martian bow shock or foreshock. A representative example is displayed in Fig. 6a. During the time interval of the magnetic field increase the electron density and temperature (not shown) also

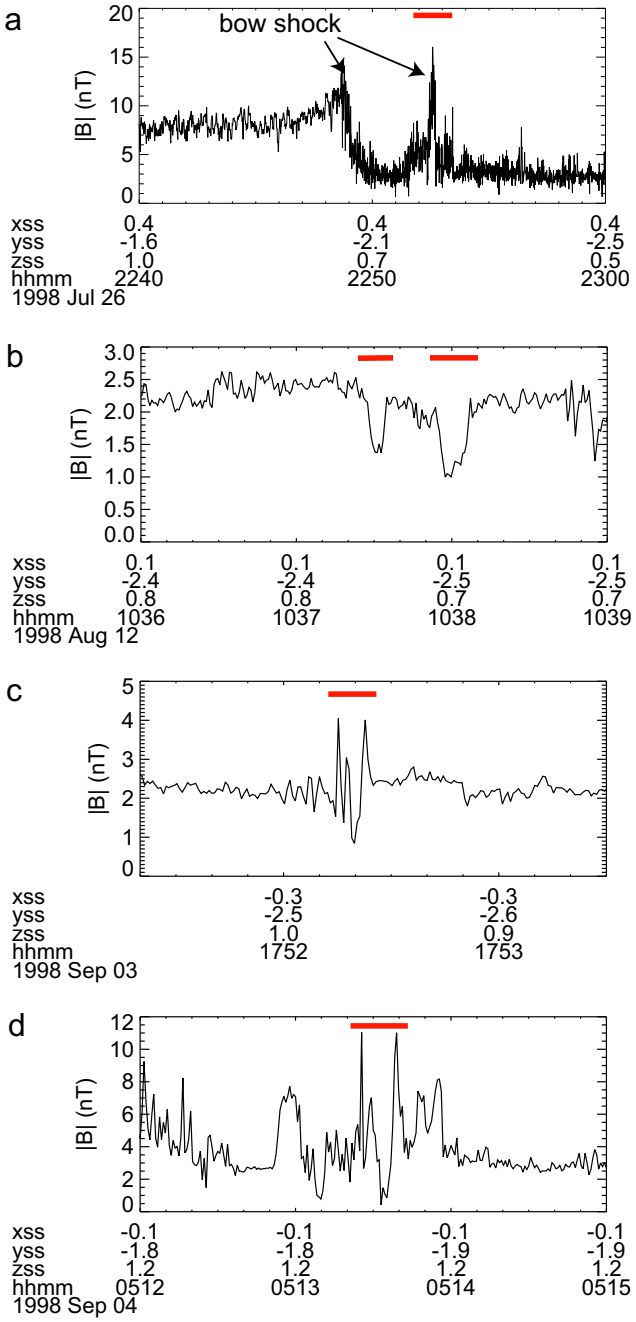

Fig. 6. Magnetic field disturbance events (marked with red lines) identified in the vicinity of the Phobos orbit: (a) example of multiple bow shock crossing observed 1800 km from Phobos' orbit, on 1998-07-26; (b) two events observed 1400 km from Phobos' orbit, on 1998-08-12; (c) event observed 700 km from Phobos' orbit, on 1998-09-03; (d) event observed 2000 km from Phobos' orbit, on 1998-09-04. The last three events show characteristics typical of foreshock cavities. (For interpretation of the references to color in this figure legend, the reader is referred to the web version of this article.)

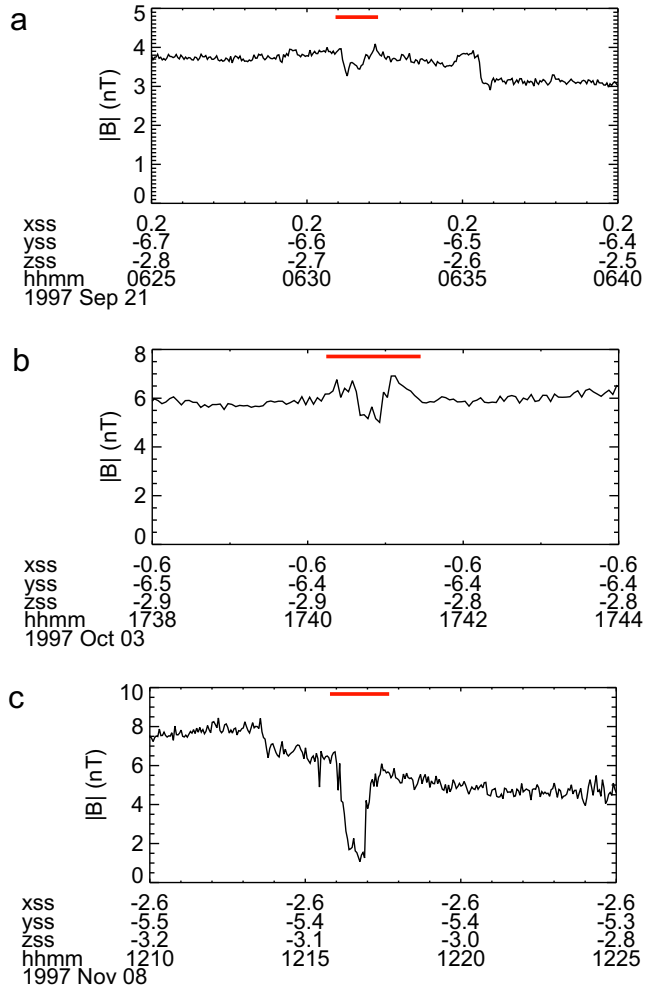

Fig. 7. Magnetic field disturbance events (marked with red lines) identified in the vicinity of the Deimos orbit: (a) event observed 1700 km from Deimos' orbit, on 1997-09-21; (b) event observed 950 km from Deimos' orbit, on 1997-10-03; (c) event observed 700 km from Deimos' orbit, on 1997-11-08. The events show characteristics typical of foreshock cavities. (For interpretation of the references to color in this figure legend, the reader is referred to the web version of this article.)

increased to levels consistent with this being a crossing into the martian magnetosheath. The four remaining events, recorded 1800 km, 1400 km, 1400 km, and 700 km from the Phobos orbit, respectively (Fig. 6b–d), all exhibited brief depressions in magnetic field magnitude, often flanked by magnetic field magnitude increases. These are features characteristic of foreshock cavities commonly observed upstream of the Earth's bow shock (Sibeck et al., 2002). Although not previously reported upstream of Mars, similar cavities are found throughout the spatial region covered by the MGS AB and SPO orbits (e.g., Fig. 2b). Hence these types of events are not confined to the Phobos orbit and are likely the martian counterpart of the terrestrial foreshock cavities (Sibeck et al., 2002).

3.2.2. Candidate "Deimos events"

Three events were identified within 2000 km of the Deimos orbit (Fig. 7). These three events were recorded 1700 km, 950 km, and 700 km from the Deimos orbit, respectively, and all events displayed brief depressions in magnetic field magnitude flanked by magnetic magnitude increases (Fig. 7a–c), suggesting that they are foreshock cavities. The latter event (Fig. 7c) coincided with a change in IMF B_z polarity (not shown), thus it is plausible that the depression in magnetic field magnitude in this event is associated with a solar wind current sheet crossing.

4. Discussion and summary

Using MGS data from 493 pre-mapping orbits we identified a total of 1246 solar wind disturbance events. As shown in Figs. 3–5, there is no preference for events to occur in the vicinity or downstream of Phobos, Phobos' orbit, or Deimos' orbit. Thus it is

likely that the 1246 events are caused by well-known solar wind or foreshock processes.

Candidate processes include foreshock turbulence (Paschmann et al., 1979; Russell et al., 1990; Skalsky et al., 1998), hot flow anomalies (Schwartz et al., 1985;Thomsen et al., 1986; Øieroset et al., 2001), and foreshock cavities (Sibeck et al., 2002). In particular the event displayed in Fig. 2a has properties that are typical of foreshock events, which can be generated when the solar wind magnetic field is connected to the martian bow shock (e.g., Russell et al., 1990). During the event shown the magnetic field briefly changed direction from being roughly parallel to the dawn flank bow shock to being almost perpendicular to it, i.e. the magnetic field was likely connected to the bow shock. The events in Fig. 2b display properties typical of foreshock cavities (Sibeck et al., 2002), with sudden and relatively brief depressions in the magnetic field magnitude. Sibeck et al. (2002) suggested that foreshock cavities are formed by diamagnetic effects of ions Fermi accelerated within the foreshock. In contrast to hot flow anomalies (HFAs) these diamagnetic cavities do not lie centered upon IMF tangential discontinuities, do not exhibit a flow deflection, and the temperature increase is less significant (Sibeck et al., 2002).

Although the processes mentioned above commonly generate solar wind disturbance events upstream of Mars the question remains whether these solar wind and foreshock processes could have dominated the statistical study to such a degree that they may have suppressed any Phobos/Deimos-related events. The Phobos-2 Phobos events were found within 700 km of the Phobos orbit. Although the occurrence frequency did not rise near the Phobos and/or Deimos orbits, we did identify eleven solar wind disturbance events within 2000 km of the Phobos orbit and three events within 2000 km of the Deimos orbit. These events were studied in detail.

Seven of the events found near Phobos' orbit were observed in the close vicinity of the martian bow shock and displayed features characteristic of bow shock crossings and/or large magnetic field amplitude foreshock fluctuations. The four remaining candidate Phobos events were observed 1800 km, 1400 km, 1400 km, and 700 km from the Phobos orbit, respectively (Fig. 6b–d) and displayed features commonly observed in terrestrial foreshock cavities (Sibeck et al., 2002), with brief depressions in magnetic field magnitude, sometimes flanked by magnetic field magnitude increases. Since foreshock cavities are found throughout the spatial region covered by MGS (e.g., Fig. 2b) we do not find any conclusive evidence that the cavities found in the vicinity of the Phobos orbit are related to outgassing or dust escape from Phobos.

Three events similar to the foreshock cavities observed near the Phobos orbit were also identified within 2000 km of the Deimos orbit (Fig. 7a–c). The three events were recorded 1700 km, 950 km, and 700 km from the Deimos orbit, respectively, and all events displayed brief depressions in magnetic field magnitude flanked by magnetic magnitude increases (Fig. 7a–c), suggesting that they are indeed foreshock cavities (Sibeck et al., 2002). However, the latter event (Fig. 7c) coincided with a change in IMF B_z polarity (not shown), thus it is plausible that the depression in magnetic field magnitude in this event is associated with the solar wind current sheet crossing.

Although a relation to Phobos and Deimos outgassing or dust escape cannot be completely discarded for the events found near the moons' orbits, the fact that the occurrence frequency does not increase near the moons' orbits combined with the fact that the events found closest to the Phobos and Deimos orbits can be explained by known solar wind processes suggest that none of the solar wind magnetic field disturbance events were caused by dust or gas along the orbits of the martian moons.

Finally, we note that if gas or dust is present along the moons' orbits the spatial distribution of magnetic field signatures could depend on the direction of the solar wind electric field. The pickup process may lead to a preference for events to occur below or above the ecliptic plane depending on the IMF direction. However, after sorting the events according to the *dx*, *dy*, and *dz* directions the event numbers are rather small (Figs. 3–5). Dividing the data even further will not yield reliable results using the current data set.

The sensitivity of the MGS magnetometer is similar to the one onboard Phobos-2 which detected the Phobos-2 Phobos events (Riedler et al., 1989; Dubinin et al., 1990). Thus if the Phobos-2 Phobos events were indeed caused by gas or dust along the Phobos orbit one would expect that the MGS MAG instrument would have been able to detect such signatures as well. The present study therefore raises the question whether the Phobos-2 Phobos events had other causes. This question has been raised previously (Russell et al., 1990; Dubinin et al., 1995). Russell et al. (1990) suggested that the Phobos-2 Phobos events were likely to be foreshock events since the magnetic field was connected to the bow shock at the time of the events. Dubinin et al. (1995) suggested that at least one of the Phobos events could be a hot diamagnetic cavity (later termed hot flow anomaly).

In summary, our study indicates that there is no preference for solar wind disturbance events to occur near the martian moons or their orbits, i.e. we find no evidence of gas/dust tori along the Phobos and Deimos orbit. The level of outgassing/dust escape from the martian moons is likely too low to give rise to magnetic field signatures detectable by MGS. Our results imply that more sensitive instrumentation, e.g. an electric field instrument or a gas/dust detector, would be needed on future spacecraft to enable in situ detection of possible low levels of gas/dust escaping the martian moons.

Acknowledgments

M. Ø. gratefully acknowledges discussions with Stas Barabash and Konrad Sauer. We also greatly appreciate the helpful comments provided by both referees. This research was supported by NASA Grant NAG5-13273 at UC Berkeley.

References

Acuña, M.H., and 19 colleagues, 1998. Magnetic field and plasma observations at Mars: Initial results of the Mars Global Surveyor mission. Science 279 (5357), 1676–1680. doi:10.1126/science.279.5357.1676.

Baumgärtel, K., Sauer, K., Dubinin, E., Tarrasov, V., Dougherty, M., 1998. Phobos events – Signatures of solar wind interaction with a gas torus? Earth Planet. Space 50, 453–462.

Blanco-Cano, X., Russell, C.T., Huddleston, D.E., Strangeway, R.J., 2001. Ion cyclotron waves near Io. Planet. Space Sci. 49 (10–11), 1125–1136.

Bogdanov, A.V., 1981. Mars satellite Deimos interaction with the solar wind and its influence on flow around Mars. J. Geophys. Res. 86, 6926.

Cowee, M.M., Russell, C.T., Strangeway, R.J., Blanco-Cano, X., 2007. One-dimensional hybrid simulations of obliquely propagating ion cyclotron waves: Application to ion pickup at Io. J. Geophys. Res. 112, A06230. doi:10.1029/2006JA012230.

Dubinin, E.M., Lundin, R., Pissarenko, N.F., Barabash, S.V., Zakharov, A.V., Koskinen, H., Schwingenschuh, K., Yeroshenko, Ye.G., 1990. Indirect evidence for a gas/dust torus along the Phobos orbit. Geophys. Res. Lett. 17, 861–864.

Dubinin, E., Obod, D., Lundin, R., Schwingenschuh, K., Grard, R., 1995. Some features of the martian bow shock. Adv. Space Res. 15 (8/9), 423–431.

Duxbury, T.C., Ocampo, A.C., 1988. Mars – Satellite and ring search from Viking. Icarus 76, 160–162.

Ip, W.-H., Banaszkiewicz, M., 1990. On the dust/gas tori of Phobos and Deimos. Geophys. Res. Lett. 17, 857–860.

Krymskii, A.M., Breus, T.K., Dougherty, M.K., Southwood, D.J., Axford, W.I., 1992. The electromagnetic effects of the solar wind interaction with the Phobos neutral gas halo and dust torus. Planet. Space Sci. 40, 1033–1041.

Mazelle, C., and 12 colleagues, 2004. Bow shock and upstream phenomena at Mars, in Mars' magnetism and its interaction with the solar wind. In: Winterhalter, D., Acuna, M., Zakharov, A. (Eds.), Space Sciences Series of ISSI, vol. 18, Kluwer Academic Publishers, p. 115 (also in Space Science Reviews, 111, 115, 2004).

Øieroset, M., Mitchell, D.L., Phan, T.D., Lin, R.P., Acuña, M.H., 2001. Hot diamagnetic cavities upstream of the martian bow shock. Geophys. Res. Lett. 28, 887–890.

Paschmann, G., Sckopke, N., Bame, S.J., Asbridge, J.R., Gosling, J.T., Russell, C.T., Greenstadt, E.W., 1979. Association of low? frequency waves with suprathermal ions in the upstream solar wind, Geophys. Res. Lett. 6 (3), 209–212.

Riedler, W., Schwingenschuh, K., Möhlmann, D., Oraevski, V.N., Eroshenko, E., Slavin, J., 1989. Magnetic fields near Mars – First results. Nature 341, 604–607.

Russell, C.T., Luhmann, J.G., Schwingenschuh, K., Riedler, W., Yeroshenko, Ye.G., 1990. Upstream waves at Mars: Phobos observations. Geophys. Res. Lett. 17, 897–900.

Russell, C.T., Kivelson, M.G., 2000. Detection of so in Io's exosphere. Science 287, 1998–1999.

Russell, C.T., Blanco-Cano, X., 2007. Ion-cyclotron wave generation by planetary ion pickup. J. Atm. Solar-terrestrial Phys. 69, 1723–1738. doi:10.1016/j.jastp.2007.02.014.

Sauer, K., Dubinin, E., Baumgartel, K., Bogdanov, A., 1995. Deimos: An obstacle to the Solar Wind. Science 269 (5227), 1075–1078.

Schwartz, S.J., Chaloner, C.P., Hall, D.S., Christiansen, P.J., Johnstones, A.D., 1985. An active current sheet in the solar wind. Nature 318, 269–271.

Showalter, M.R., Hamilton, D.P., Nicholson, P.D., 2006. A deep search for martian dust rings and inner moons using the Hubble Space Telescope. Planet. Space Sci. 54, 844–854.

Sibeck, D.G., Phan, T.-D., Lin, R., Lepping, R.P., Szabo, A., 2002. Wind observations of foreshock cavities: A case study. J. Geophys. Res. 107, 1271. doi:10.1029/2001JA007539.

Skalsky, A., Dubinin, E., Delva, M., Grard, R., Klimov, R.S., Sauer, K., Trotignon, J.-G., 1998. Wave observations at the foreshock boundary in the near-Mars space. Earth, Planets Space 50, 439–444.

Soter, S., 1971. The Dust Belts of Mars, Center for Radiophysics and Space Research, CRSR 462, Cornell University.

Thomsen, M.F., Gosling, J.T., Fuselier, S.A., Bame, S.J., Russell, C.T., 1986. Hot, diamagnetic cavities upstream from the Earth's bow shock. J. Geophys. Res. 91, 2961–2973.

Tokar, R.L., and 10 colleagues, 2006. Cassini detection of water-group pick-up ions in the Enceladus torus. Geophys. Res. Lett. 35, L14202. doi:10.1029/2008GL034749.